

Void Analysis of Hadronic Density Fluctuations at Phase Transition

Rudolph C. Hwa¹ and Qing-hui Zhang²

¹Institute of Theoretical Science and Department of Physics
University of Oregon, Eugene, OR 97403-5203, USA

²Physics Department, McGill University, Montreal QC H3A 2T8, Canada

Abstract

The event-to-event fluctuations of hadron multiplicities are studied for a quark system undergoing second-order phase transition to hadrons. Emphasis is placed on the search for an observable signature that is realistic for heavy-ion collisions. It is suggested that in the 2-dimensional y - ϕ space the produced particles selected in a very narrow p_T window may exhibit clustering patterns even when integrated over the entire emission time. Using the Ising model to simulate the critical phenomenon and taking into account a p_T distribution that depends on the emission time, we study in the framework of the void analysis proposed earlier and find scaling behavior. The scaling exponents turn out to be larger than the ones found before for pure configurations without mixing. The signature is robust in that it is insensitive to the precise scheme of simulating time evolution. Thus it should reveal whether or not the dense matter created in heavy-ion collisions is a quark-gluon plasma before hadronization.

1 Introduction

It is well known that a system undergoing a second-order phase transition exhibits large fluctuations and long-range correlations. If the symmetry of a quark system created in a heavy-ion collision is such that the quark-hadron phase transition is second order, then one would expect large fluctuations in the multiplicity of hadrons produced, not only from event to event (which happens normally in high-energy collisions), but also from one region to another in the geometrical space into which the particles are emitted at any given time. It is the latter type of fluctuations that we focus on as a possible signature of the phase transition, when an appropriate measure can be identified.

The fluctuation of local hadron density implies the formation of spatial patterns that exhibit clusters of hadrons of varying sizes. There are also regions of no particles, which are referred to as voids. An investigation of the fluctuation of void sizes was carried out by

us recently in Ref. [1]. We found scaling behaviors, whose exponents were proposed as an observable signature of quark-hadron phase transition (PT).

Recently an analysis of the NA49 data on $Pb-Pb$ collisions at CERN-SPS was carried out according to the method described in Ref. [1]. It is found [2] that the scaling behaviors exist under certain restricted conditions of the analysis, and that the scaling exponents are significantly lower than the ones predicted in [1].

The void analysis studied in [1] has its limitations. The most serious shortcoming is that it is an analysis of a system that is essentially static. The aim has been to find a measure suitable for quantifying effectively a given spatial pattern, or a set of them. However, the hadronization process in a heavy-ion collision is dynamical and takes place over an extended period of time. If the particles emitted throughout the whole duration are collected at every local region, then the patterns examined in the static scenario overlap one another, and the fluctuating patterns would disappear in the cumulative result.

An analogy to this problem is the nature of rainfalls in two geographical regions with very different climates. It is not possible to judge from their annual precipitations (assuming that they are roughly the same) whether the rain in one region is stormy, or the other drizzly. It is necessary to make cuts in the time duration to learn about the spatial fluctuations in short time intervals. Similarly, in heavy-ion collisions it would be ideal if we could select a small Δt interval to analyze the spatial pattern of an event. That is, however, not feasible in a heavy-ion experiment. The only cut that can be made experimentally while keeping the $y-\phi$ space for analysis is in the p_T variable, i.e., selecting particles in a small Δp_T interval. How to prepare the spatial configuration for our analysis in a way that corresponds to how the experimental data are to be analyzed is an essential part of the present work.

As in [1], which follows the theoretical framework of Ref. [3], we assume that the dense quark matter created in a heavy-ion collision is cylindrical in shape, expanding rapidly in the longitudinal direction and more gradually in the radial direction. It is further reasonable to assume that the thermal system is hot on the inside (with $T > T_c$) and cooler on the surface, where at $T \simeq T_c$ the plasma undergoes a PT to hadrons. Thus the critical phenomenon occurs on a two-dimensional surface with the particle momenta being mainly normal to that surface. The fluctuation that we want to examine is in the hadron density from region to region in the $y-\phi$ space for particles that are emitted in a small p_T interval. To simulate that fluctuation we make use of the theoretical result that the phase boundary between a first-order PT for some low quark masses and a crossover at higher quark masses is a second-order PT belonging to the same universality class as the Ising system [4, 5]. We map a section of the $y-\phi$ space on the surface of the plasma cylinder created in a heavy-ion collision to a 2D Ising lattice. We use the Ising model to simulate the spatial pattern of clusters of spins pointing in the same direction, and relate a cell with a net spin pointing in one direction to a hadron, and a cell with a net spin in the other direction to no-hadrons, i.e., locally and temporarily still in the quark state. That is the model that we have used in [1, 3], the essential part of which will be summarized in Sec. 2.

Regarding what is simulated on the Ising lattice as a representation of the hadrons density fluctuation on the surface of the plasma cylinder at any given time, we have to relate that to the experimental situation of particles collected in a Δp_T cut, but accumulated throughout the entire hadronization time that can exceed 10 fm/c. It is a problem of preparing the temporally-integrated configuration on the lattice that can best approximate the real data.

The problem will be discussed in Sec. 3. The analysis of the mixed configurations that leads to scaling behaviors is the content of Sec. 4.

2 Simulation and Analysis of Hadronic Density Fluctuation

An essential feature of critical behavior is that the critical exponents of different systems belong to the same universality class if the systems have the same symmetry and dimension [6]. Our use of the Ising model to simulate the spatial patterns at PT is based on the recognition that for appropriate masses of the light and strange quarks the quark-hadron PT is in the same universality class as the Ising system [4, 5]. That is fortunate, since the simulation of Ising lattice is extremely simple. However, the realistic quark masses may not have exactly the values that correspond to the ones on the phase boundary where the second-order PT occurs. It is highly likely that the realistic point in the phase diagram is in the broad region of a crossover above the boundary line characterized by the Ising system. Fortunately again, a crossover can also be easily simulated on the Ising lattice by providing a preferred direction for the spins to be aligned. We summarize here the main points in the relationship between the Ising problem and the hadron density problem, and then outline the void analysis, the details of which can be found in [1].

For a 2D lattice of size L^2 with each site having spin $\sigma_j = \pm 1$, we define the spin aligned along the overall magnetization $m_L = \sum_{j \in L^2} \sigma_j$ by

$$s_j = \text{sgn}(m_L)\sigma_j \quad , \quad (1)$$

where $\text{sgn}(m_L)$ stands for the sign of m_L . We relate hadronization at location i to a cell of size ϵ^2 with net spin c_i positive, where

$$c_i = \sum_j s_j \quad , \quad (2)$$

with the sum being over all sites in the cell. If $c_i \leq 0$, no hadronization takes place at i . Hadron density is defined by

$$\rho_i = \lambda c_i^2 \theta(c_i) \quad , \quad (3)$$

where λ is an unspecified factor relating the lattice spins to the number of particles per unit area in y - ϕ space. The scaling behavior to be examined should, of course, be independent of the normalization factor λ .

Since lattice spins fluctuate from site to site when T is near T_c , ρ_i also fluctuates from cell to cell, either positive or zero. When averaged over all cells of a configuration, and then averaged over all uncorrelated configurations at any given T , $\langle \rho \rangle$ is a smooth function of T , descending rapidly near T_c as T is increased [1, 3]. It is a crossover, since the first few orders of derivatives exhibit no signs of discontinuities. The value of T_c is determined by examining the scaling behavior of the normalized factorial moments F_q [7], and is found to be $T_c = 2.315$ in the Ising model units of J/k_B .

In practice we work with a lattice having $L = 288$ and cells of size $\epsilon = 4$. For scaling behavior we study the dependences of our measures on the bin size $\delta \times \delta$. The average hadron density in a bin is $\bar{\rho}_b = \nu^{-1} \sum_{i=1}^{\nu} \rho_i$, where $\nu = (\delta/\epsilon)^2$. Near T_c , $\bar{\rho}_b$ fluctuates from bin to bin, especially for small δ . It is that fluctuation we want to characterize by quantitative measures. Our proposal is to represent $\bar{\rho}_b$ in the 2D space by topographical maps with various discrete elevations ρ_0 . For every given ρ_0 we define a bin to be “empty” when

$$\bar{\rho}_b < \rho_0 \quad . \quad (4)$$

and further define a void to be a collection of contiguous empty bins, connected by at least one side between neighboring bins. An analogy for this analysis is to flood a rough terrain by water and characterize the landscape profile by either land (nonempty bin) or water (empty bin). Clearly, by studying the areas of the submerged regions at different water levels, one can capture the topographical properties of the terrain. In our problem the maximum possible value of ρ_i in a cell is $(\epsilon^2)^2 = 256$ in units of λ . A range of ρ_0 between 20 and 100 have been used in our void analysis in [1].

For the void analysis let V_k be the size of the k th void in units of bins

$$V_k = \sum_{\langle b \rangle_k} \theta(\rho_0 - \bar{\rho}_b) \quad , \quad (5)$$

where the sum is over all empty bins in the k th void. Then, let $x_k = V_k/M$ be the fraction of bins in the lattice occupied by V_k , where $M = (L/\delta)^2$ is the total number of bins, and let m be the total number of voids in the configuration. We define the normalized G moments to be

$$G_q = \frac{1}{m} \sum_{k=1}^m x_k^q \bigg/ \left(\frac{1}{m} \sum_{k=1}^m x_k \right)^q \quad . \quad (6)$$

For every given configuration, G_q can be determined for various bin sizes, i.e., as a function of M . G_q can fluctuate widely from configuration to configuration. That fluctuation can be described by a probability distribution $P(G_q)$. While many moments of that distribution can be studied, we have proposed the two lowest moments

$$\langle G_q \rangle = \int dG_q G_q P(G_q) \quad , \quad (7)$$

$$S_q = \langle G_q \ln G_q \rangle \quad , \quad (8)$$

the latter being the derivative with respect to p of the p th moment evaluated at $p = 1$ [1].

For pure configurations simulated on the Ising lattice, scaling behaviors have been found for both $\langle G_q \rangle$ and S_q

$$\langle G_q \rangle \propto M^{\gamma_q} \quad , \quad (9)$$

$$S_q \propto M^{\sigma_q} \quad , \quad (10)$$

for a range of values of ρ_0 [1]. Furthermore, γ_q and σ_q depend on q linearly as

$$\gamma_q = c_0 + cq \quad , \quad (11)$$

$$\sigma_q = s_0 + sq \quad . \quad (12)$$

Thus the values c and s (which are the slopes of slopes) are concise characterizations of the fluctuation behavior near the critical point.

It should be stressed that although the 2D Ising model can be solved exactly for an infinite system[8], the conventional description of its critical behavior is in terms of the temperature T in the vicinity of T_c . For a quark-hadron system created in a heavy-ion collision, T is not measurable, nor controllable. Our proposed measures of the critical behavior can be determined in high-energy nuclear experiments without any knowledge about T .

3 Mixed Configurations for an Evolving System

In the previous section we described the observable measures that can be applied to the heavy-ion data on the one hand, and can extract salient features of critical configurations on the other. Now we focus on the issue of preparing the configurations that correspond more closely to the realistic situation of a quark-gluon plasma expanding, cooling, and hadronizing.

While a detailed modeling of the hydrodynamical expansion of a quark-gluon system is inappropriate for our purpose here, we can emphasize the main features of such an expanding system and incorporate them in our preparation procedure. Our assumption is that the temperature profile of the plasma cylinder is such that T is high ($> T_c$) in the interior and decreases monotonically toward the surface until T_c , where quark-hadron PT takes place at the surface. The hadrons are emitted nonuniformly from the surface with transverse momenta p_T that can be measured for each particle. The average $\langle p_T \rangle$ depends on the radial pressure gradient, which in turn depends on time, since the longitudinal expansion lowers the temperature throughout the cylindrical interior and the radial expansion lowers the radial pressure gradient. Disregarding high- p_T hard scattering, which affects $\langle p_T \rangle$ only in a minor way, we may take the general hydrodynamical implication to be that $\langle p_T \rangle$ decreases with the pressure gradient, and therefore with the evolution time t .

If the p_T distribution at any given time were narrow, but when integrated over all times it gives the usual exponential damping in p_T for the event distribution dN/dp_T , then our problem would be simple. In the idealized situation of a one-to-one correspondence between p_T and t , a narrow Δp_T cut in p_T would result in a narrow Δt cut in emission time. That would provide us with a narrow temporal window to view the spatial pattern of hadronization activities on the cylinder surface, and the pure configurations simulated on the Ising lattice would suffice to model the effects of the critical behavior, as discussed in the previous section.

The reality is, however, quite the opposite. At any given t the p_T distribution is broad, so the particles emitted into a small Δp_T interval can come from a wide range of t . That introduces a complication related to the correlation between successive emission times. But, first, let us describe the p_T - t correlation by a model formula that captures the essence of

the hydrodynamical character of the p_T distribution at different times [9]. We adopt the Gaussian formula

$$P(p_T, t) = N(t)\exp\{-[p_T - p_0(t)]^2/2p_0^2(t)\} \quad , \quad (13)$$

where

$$p_0(t) = 2/t \quad \text{GeV}/c \quad (14)$$

and $N(t)$ is the normalization factor that preserves the condition

$$\int dp_T P(p_T, t) = 1 \quad (15)$$

for all $t \geq 1$. It is clear that, as t increases, the Gaussian peak shifts toward lower p_T and its width also decreases correspondingly. If we make a narrow Δp_T cut, say $0.3 < p_T < 0.35$ GeV/c, there are contributions from a wide range of t that are not negligible.

We note that the accuracy of Eq. (13) is not important for our purpose, since firstly the p_T distribution depends on the evolution model and on many parameters in the initial condition, and secondly we use it only for simulating configurations at different times in the evolution process in the framework of the Ising model, which is a simple generator of PT configurations that ignore the realistic complications of surface irregularity, quark density fluctuations, surface tension, etc. However, Eq. (13) does contain the essence of overlapping p_T distributions at successive times, a feature that we want to incorporate in our simulation. The variable t in Eqs. (13) and (14) is used only in the sense of representing time in the simulation (to be detailed below), not as real time in heavy-ion collisions in some physical unit. We emphasize that the correspondences between the lattice variables and realistic quantities in heavy-ion experiments have never been fixed. In Eq. (3) we did not specify λ that relates lattice spins to hadron density; the scaling behaviors we seek are independent of λ . Here we similarly do not know how to specify the precise relationship between the number of steps in the evolution of the Ising lattice and the actual time of hydrodynamical evolution of a quark system. We now consider how many steps to take.

If at any given t we have on the Ising lattice a configuration of hadrons and voids, then it is very reasonable to expect that at 1 fm/c later in real time the previous void-region will have a higher probability to hadronize than the region where hadronization has already occurred. Of course, there are fluctuations in local temperature, in surface curvature, pressure gradient, quark density, and other local properties of the statistical and collective system, all of which are unknown and can affect hadronization locally. Our procedure is primarily to let the Ising system evolve by updating the spin configuration using the Wolff logarithm [10]. Let S denote the number of steps of updating the Ising spin orientations that corresponds to 1 fm/c in real time. Not knowing what S is, but realizing that the Ising configuration does not change drastically in one or two steps, we adopt the following two options.

Option 1. $S = 5$

After every five steps of updating the Ising configuration, we reverse the direction of what is “up” to allow the cells in the void region in the previous configuration to be preferred for hadronization. That is, denoting the number of Ising steps by nS , we let $t = n$ in Eq. (13), and replace Eq. (1) by

$$s_j = (-1)^n \text{sgn}(m_L) \sigma_j. \quad (16)$$

Note that if S were 1, and the Ising configuration changes very slowly, then Eq. (16) applied to (2) and (3) would suggest that $\rho_i > 0$ and $\rho_i < 0$ regions approximately alternate as n increases. That is an extreme scenario. By letting $S = 5$, we allow statistical readjustment of the lattice spins as time progresses. The $(-1)^n$ factor in (16) is put in by hand to take into account the hydrodynamical feature that any quark region is likely to hadronize at a later time due to radial expansion and cooling.

Option 2. $S = 50$

After fifty steps it is likely that some of void regions will have evolved to contain $\rho_i > 0$ cells. It is then not necessary to impose sign flip by hand, so we can continue to use Eq. (1) for s_j and rely on the fluctuations of the Ising spins to generate new configuration that correspond to successive emission time. That is, with the number of Ising steps being nS , we use $t = n$ in Eq. (13), and without the $(-1)^n$ factor in (16) we proceed with the evolution process. This is an option representing a scheme quite different from the one above.

We now describe the algorithm for generating the temporally-integrated configurations (TIC) in either option of identifying t . At each t we simulate on the Ising lattice a pattern of hadrons and voids. Let us call that a frozen configuration. At the location of every cell where $\rho_i > 0$, we assign a value of p_T according to the distribution $P(p_T, t)$ given in Eq. (13). We choose to keep only those particles whose p_T fall within the interval Δp_T that we select, say $0.3 < p_T < 0.35$ GeV. The cell location of each of those selected particles are recorded in a new configuration, which is to become the TIC. Now let t increase by one step, repeat the above procedure, and enter more particles into the TIC at the cell positions where the selected hadrons are located. We continue to do this up to t_m steps, when the accumulated particles at various places in the 2D space constitute our final TIC for that sum. The value of t_m is determined by the requirement that the average hadron density for the whole lattice is approximately equal to that in the frozen case (no t evolution and any p_T) at the same temperature T . In this way we generate a TIC, starting always with $t = 2$ so that $p_0(t)$ ranges from 1 down to 0.1 GeV/c.

For our analysis in the next section, we use a lattice of size $L = 288$, with cells of size $\epsilon = 4$, and bin sizes varying from $\delta = 8$ to 32. We select Δp_T to be between 0.2 to 0.3 GeV/c, and the corresponding t_m turns out to be 9. We generate 5×10^3 configuration for each sample for analysis, using both options for t evolution.

4 Scaling Behaviors of the Temporally-Integrated Configurations

Having described how the TIC are prepared, we proceed directly to the analysis discussed in Sec. 2 and present the results here.

Although the simulation can be done at any T in the vicinity of T_c and the analysis can be done at any elevation ρ_0 , we show only the scaling behaviors for $T = T_c$ and $\rho_0 = 40$ [in units of λ in Eq. (3)]. We shall consider both options of t evolution discussed in the previous section and label the corresponding figures by either $S = 5$ or $S = 50$.

In Fig. 1(a) we show $\langle G_q \rangle$ vs M in log-log plot for $S = 5$. Clearly, it exhibits very good scaling behavior for all values of q considered. It means that voids of all sizes exist in the

TIC. Since the behavior is very similar to the one found in [1] for the pure or frozen configurations, the implication is that the mixing of configurations selected in the Δp_T window and integrated over the emission time does not lead to a homogenization of the clustering patterns. This behavior is possible only if each of the underlying (frozen) configuration exhibits critical fluctuation. Taking a small portion of each of such configurations at different t and adding them up retain the fluctuating nature of the void structure that gives rise to the scaling behavior. This is a very fortunate feature that makes possible the detection of the critical behavior in heavy-ion collision.

From the slopes of the straight-line fits in Fig. 1(a), which are denoted by γ_q in Eq. (9), we show the dependence of γ_q on q in Fig. 1(b). Evidently, Eq. (11) is a good description of that linear dependence. The slope c of slopes is a numerical characterization of the scaling behavior of $\langle G_q \rangle$. Its value in this case is $c = 0.92$, which is significantly larger than the value of 0.7 found in [1] for pure (frozen) configurations.

The same analysis is carried out in option 2 of t evolution. The corresponding results are shown in Figs. 2(a) and (b). The value of $c = 0.97$ is slightly larger, but is sufficiently close to the value from option 1 that one can reasonably infer the essential independence of the critical fluctuation on the procedure of simulating the temporal evolution.

We have also investigated the dependences on ρ_0 . In Fig. 3 we show the values of c for the two options in t evolution as functions of ρ_0 . It should be understood that by giving the values of c we are asserting the existence of scaling such as those shown in Figs. 1(a) and 2(a) for all the values of ρ_0 examined. No essential difference between the two options of time evolution has been found. The feature in Fig. 3 to be noted is the wide range of ρ_0 from 40 to 100 in which the scaling behavior can be found. To give a sense of the normalization for those numbers, it should be remarked that the average $\langle \rho \rangle$ is around 78. That feature and the values of c ranging between 0.75 and 0.96 may now be regarded as the quantitative signature of quark-hadron phase transition that should be checked in heavy-ion collisions.

For all that have been done for $\langle G_q \rangle$ above, we can do the same for S_q defined in Eq. (8). Fig. 4(a) shows the scaling behavior of S_q vs M , whose exponents σ_q are shown in Fig. 4(b), all for $S = 5$. The value of the slope s , defined in Eq. (12), is 0.82 and $\rho_0 = 40$. For $S = 50$ the corresponding figures are shown in Figs. 5(a) and (b), and the value of s is 0.89. Finally, the dependence of s on ρ_0 is shown in Fig. 6. The range of ρ_0 is the same as for $\langle G_q \rangle$, and the range of s is between 0.7 and 0.9.

For a rough comparison we mention that in the real data of NA 49 the scaling behaviors of $\langle G_q \rangle$ and S_q are found only in very restricted ranges of ρ_0 and the values of c and s are significantly lower [2].

For comparison, we have also performed the void analysis on randomly generated statistical configurations. We have chosen two methods to generate such configurations.

Method 1. We use random-number generator to assign a value of ρ_i between 0 and 160 at site i , for i ranging over all sites on the lattice. We choose that range because the average value of ρ_i simulated in the foregoing at T_c is around 78. We collect 5×10^3 such configurations and call them the random sample.

Method 2. Generate first a configuration on the $L \times L$ sites of the lattice in the Ising model as in [1]. Choose randomly a cell i and transfer the hadron density ρ_i there to a *new* configuration at the same cell location i . Repeat this procedure $(L/\epsilon)^2$ times, each time starting with a new uncorrelated configuration; furthermore, each time the transfer

of ρ_j is made to the j th cell of the same *new* configuration. At the end of the $(L/\epsilon)^2$ th transfer, we have completed the construction of a *new* configuration, which is regarded as a mixed configuration. Then we start afresh and generate a new mixed configuration, adding to what we call the statistical sample. Specifically, we use $L = 288$ and $\epsilon = 4$. There are no correlations among the various cells in these configurations, although the underlying dynamics that generates the original configurations is that of the Ising model.

The results of our void analysis on the random and statistical samples are very similar. Scaling behavior is not found until ρ_0 is nearly as large as the mean density and then only for a narrow range of ρ_0 between 60 and 80. This is very different from our results shown in Figs. 3 and 6 that have a wide range of ρ_0 in which the scaling behavior exists, beginning with $\rho_0 \approx \langle \rho \rangle / 2$.

Based on the above results we believe that dynamically generated critical behavior in the experimental data can be distinguished from the statistical background.

5 Conclusion

What we have demonstrated in this work is that critical fluctuation in quark-hadron phase transition can be observable in heavy-ion collisions, when appropriate measures are sought for in the data analysis. The details of how we have simulated the configurations are not as important as the insistence that a narrow Δp_T cut be made. There is no chance that the experimental data at RHIC can reveal any evidence of the pattern formation in hadron density if such a cut in p_T is not applied. Scaling behavior is the canonical characteristics of critical phenomena, so to discover its existence in the data of heavy-ion collisions should be a primary area of investigation for the signatures of quark-gluon plasma. Since temperature is not directly measurable, and fluctuations in multiplicities do not manifest themselves naturally as in critical opalescence, our task is nontrivial and must rely on the identification of observables that are carefully constructed to reveal the scaling properties. Of course, if scaling is not found in the data, it could be that the phase transition is of first order, or is a crossover of such smoothness that no interesting fluctuations exist. The application of our method of analysis to the data can at least shed some light on the nature of the phase transition.

There is a possibility that scaling behavior may exist even in the absence of a second-order PT of the type discussed here. Such a possibility has been proposed earlier [11] as a manifestation of self-organized criticality [12]. Although the scaling discussed there is in terms of cluster sizes, there is no doubt that a void analysis can detect its signals, if it exists. The method proposed here should be sensitive to any hadronization process that does not produce particles uniformly in a short time interval. Application of the method to the RHIC data should be revealing whether or not scaling behavior can be found.

Acknowledgment

One of us (RCH) wishes to acknowledge Dr. Pasi Huovinen for his willingness to perform certain hydrodynamical calculations and to transmit the results to us before publication. We are grateful to Prof. C. B. Yang for communicating to us the preliminary result of his analysis of the NA49 data. This work was supported, in part, by the U. S. Department of Energy under Grant No. DE-FG03-96ER40972, the Natural Science and Engineering Research Council of Canada and the Fonds FCAR of the Quebec Government.

References

- [1] R. C. Hwa, and Q. H. Zhang, *Phys. Rev. C* **62**, 054902 (2000).
- [2] C. B. Yang, preliminary report (private communication).
- [3] R. C. Hwa, and Y. F. Wu, *Phys. Rev. C* **60**, 054904 (1999).
- [4] S. Gavin, A. Gocksch, and R. D. Pisarski, *Phys. Rev. D***49**, 3079 (1994).
- [5] K. Rajagopal, in *Quark-Gluon Plasma 2*, edited by R. C. Hwa, (World Scientific, Singapore, 1995).
- [6] N. Goldenfeld, *Lectures on Phase Transitions and Renormalization Group*, (Addison-Wesley Publ. Co., 1992)
- [7] Z. Cao, Y. Gao and R. C. Hwa, *Z. Phys. C* **72**, 661 (1996).
- [8] K. Huang, *Statistical Mechanics*, 2nd edition (Wiley & Sons, Inc., New York, 1987).
- [9] P. Huovinen (private communication).
- [10] U. Wolff, *Phys. Rev. Lett.* **62**, 361 (1989).
- [11] R. C. Hwa, C. S. Lam, and J. Pan, *Phys. Rev. Lett.* **72**, 820 (1994); R. C. Hwa and J. Pan, *Phys. Rev. C* **50**, 2516 (1994).
- [12] P. Bak, C. Tang and K. Wiesenfeld, *Phys. Rev. A* **38**, 364 (1988).

Figure Captions

Fig. 1 Option 1 in time-evolution, $S = 5$: (a) Scaling behavior of $\langle G_q \rangle$, (b) Dependence of the scaling exponent γ_q on q .

Fig. 2 Option 2 in time-evolution, $S = 50$: (a) Scaling behavior of $\langle G_q \rangle$, (b) Dependence of the scaling exponent γ_q on q .

Fig. 3 Dependences of c on ρ_0 for the two options.

Fig. 4 Option 1 in time-evolution, $S = 5$: (a) Scaling behavior of S_q , (b) Dependence of the scaling exponent σ_q on q .

Fig. 5 Option 2 in time-evolution, $S = 50$: (a) Scaling behavior of S_q , (b) Dependence of the scaling exponent σ_q on q .

Fig. 6 Dependences of s on ρ_0 for the two options.

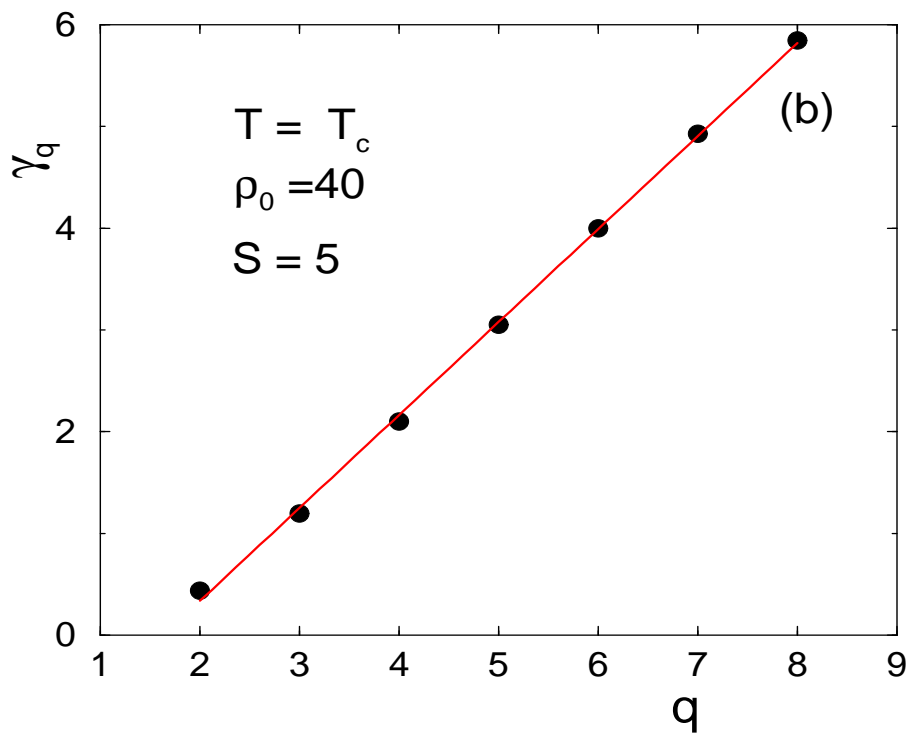
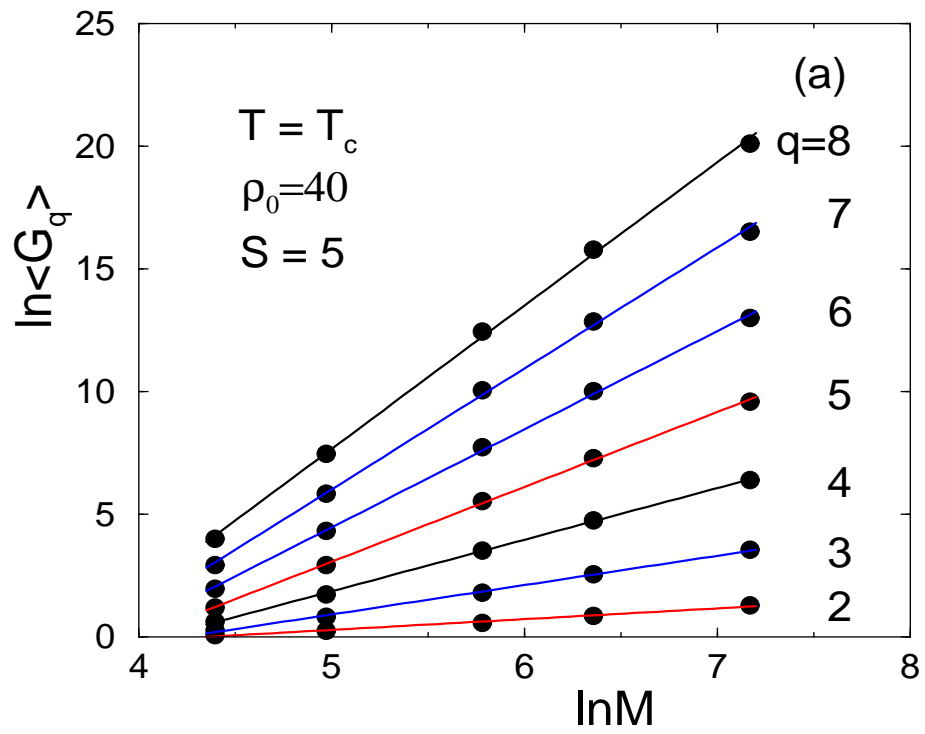


Fig.1

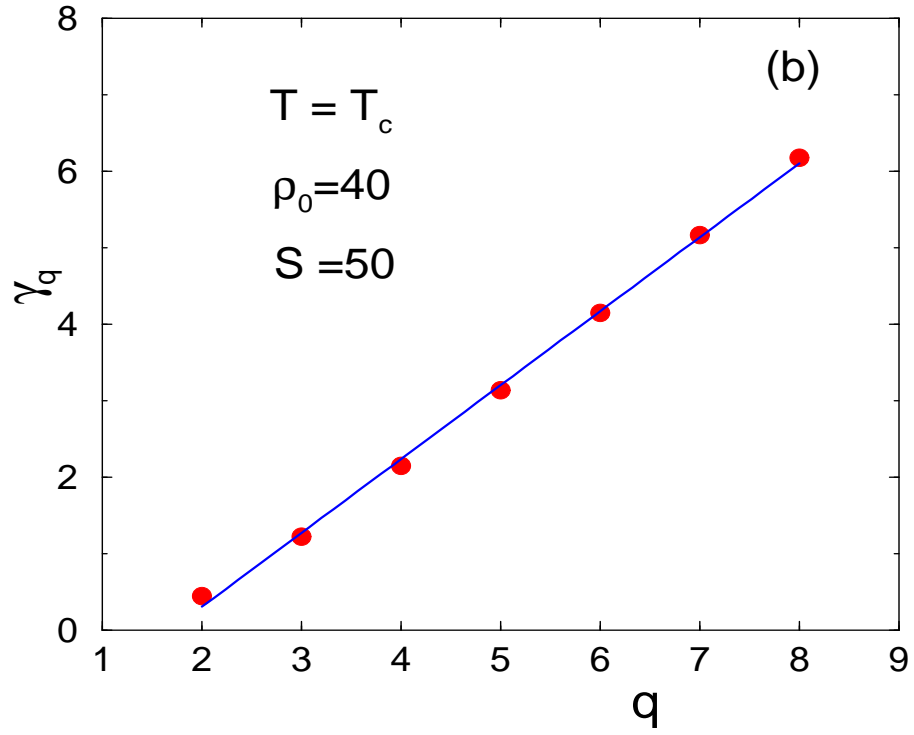
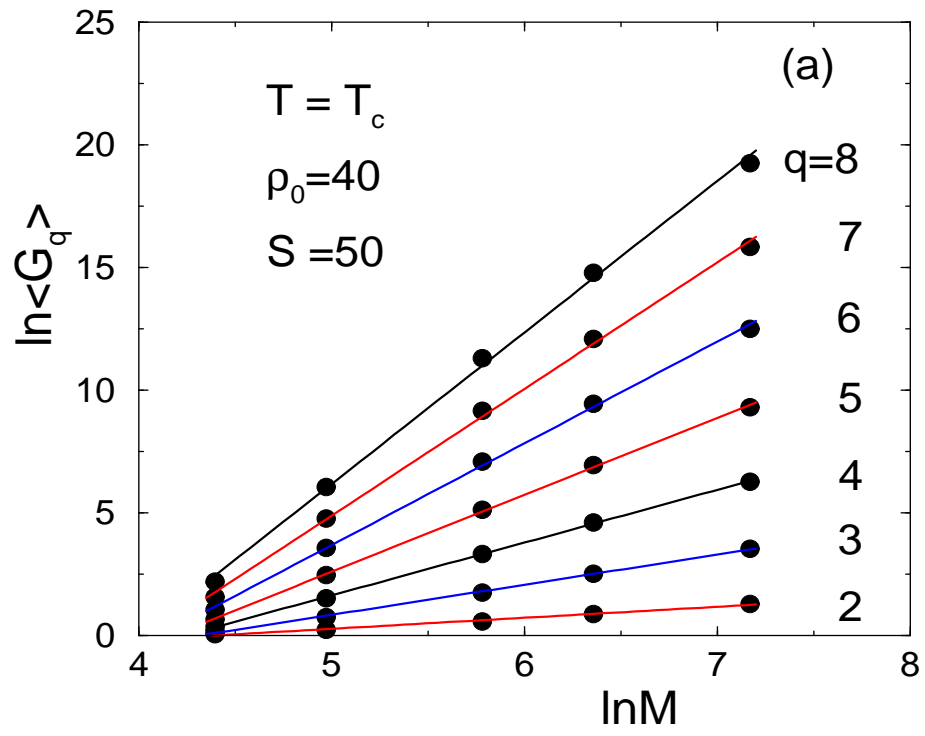


Fig.2

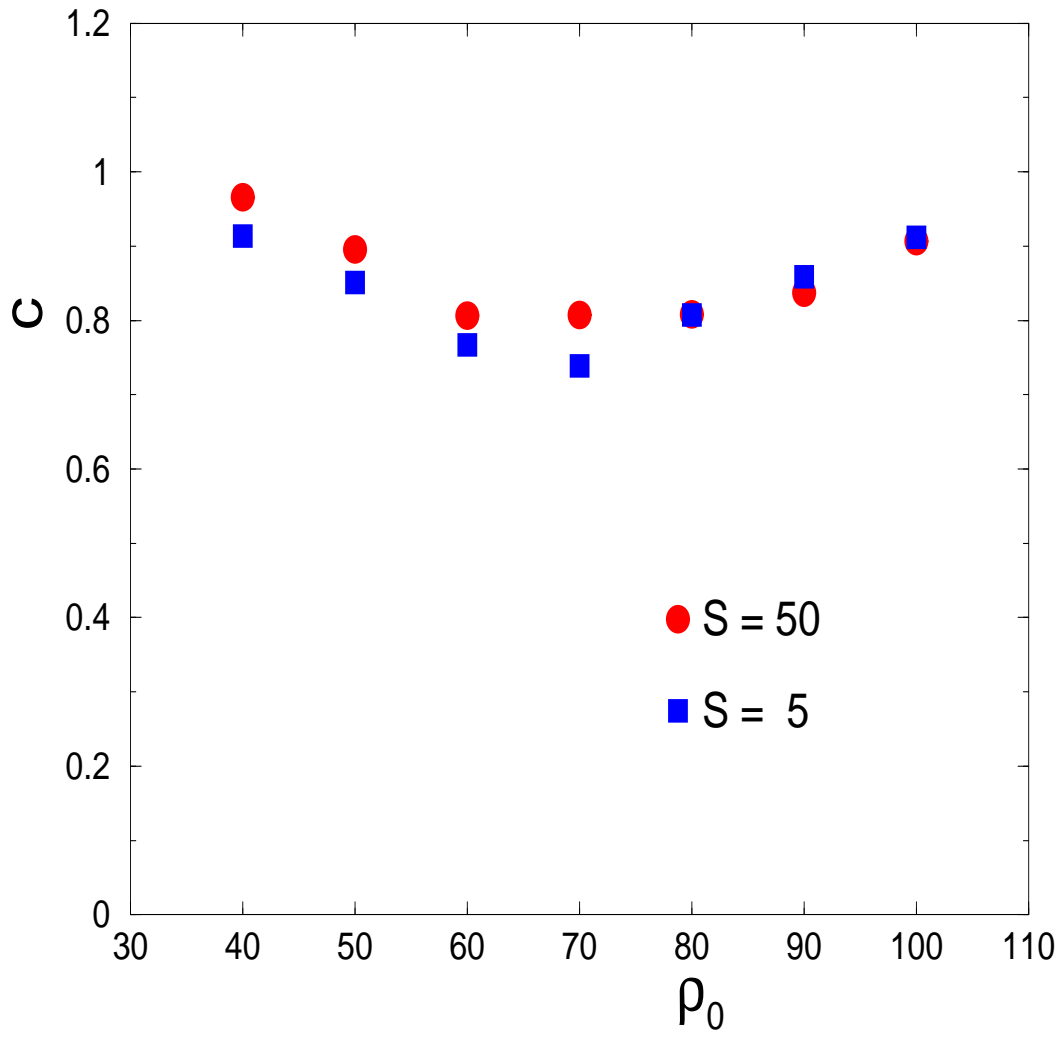


Fig.3

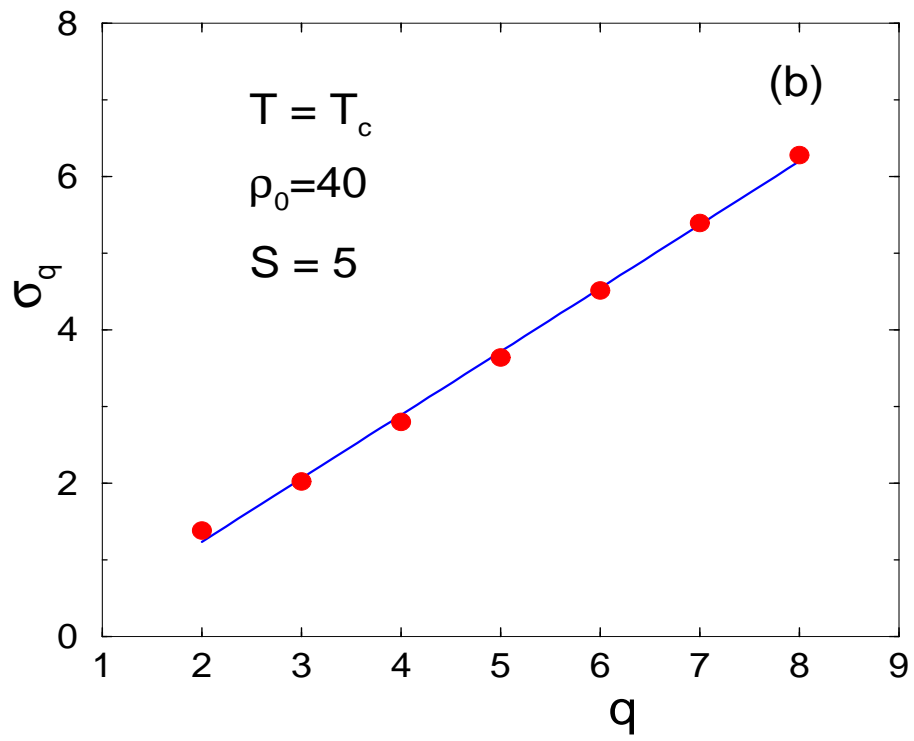
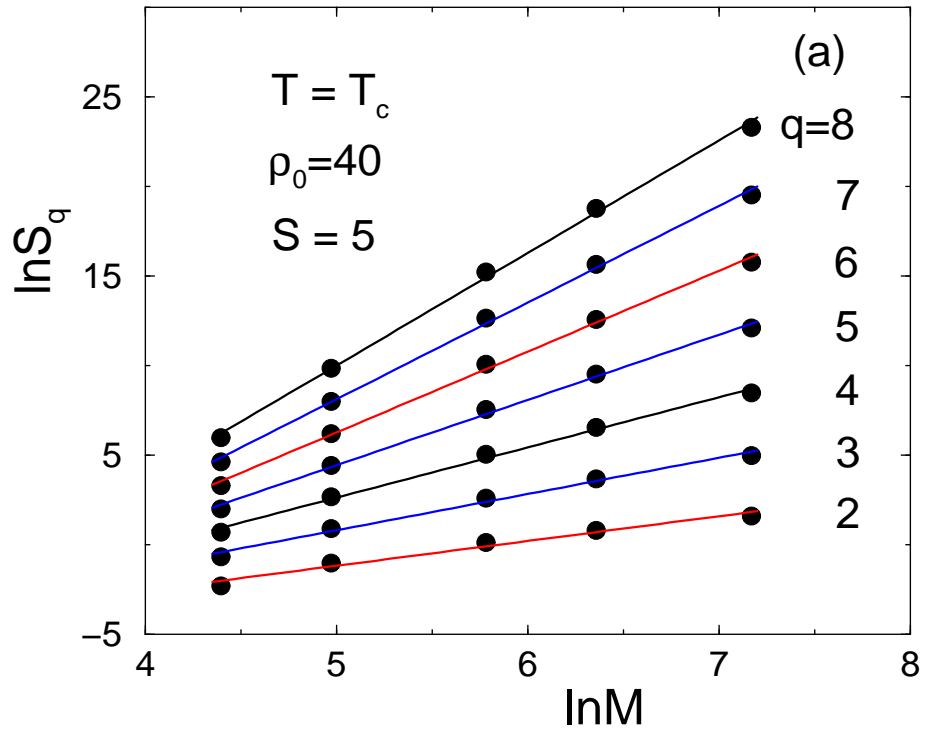


Fig.4

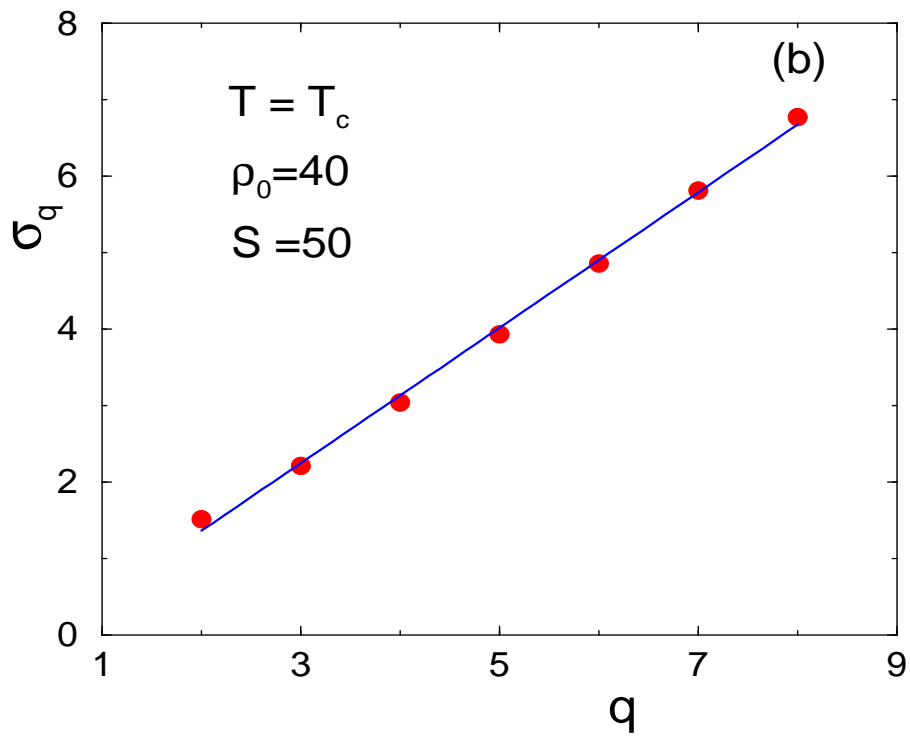
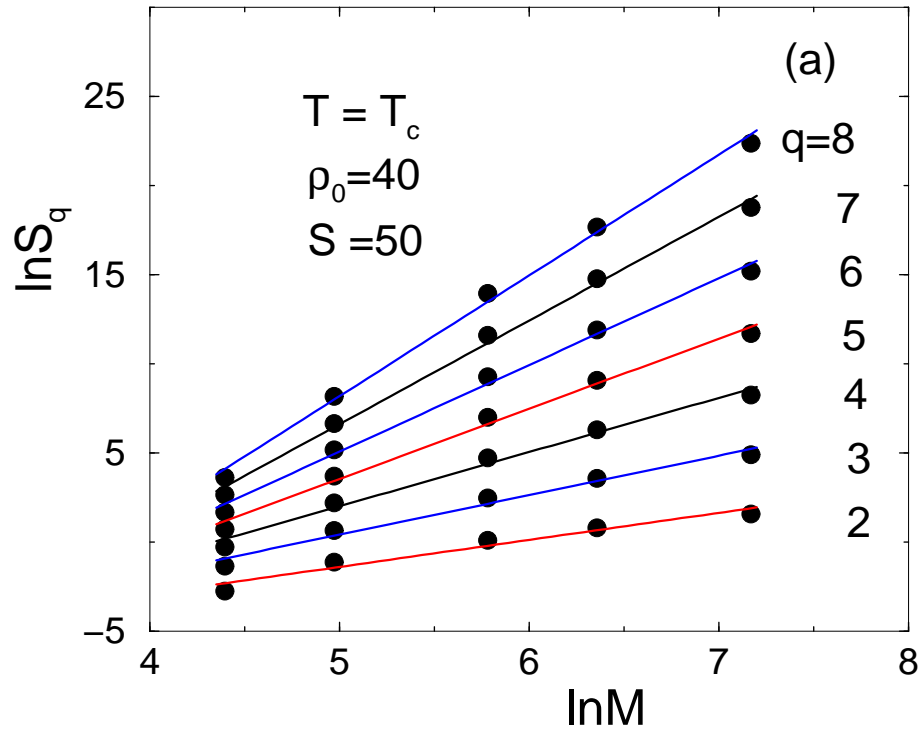


Fig.5

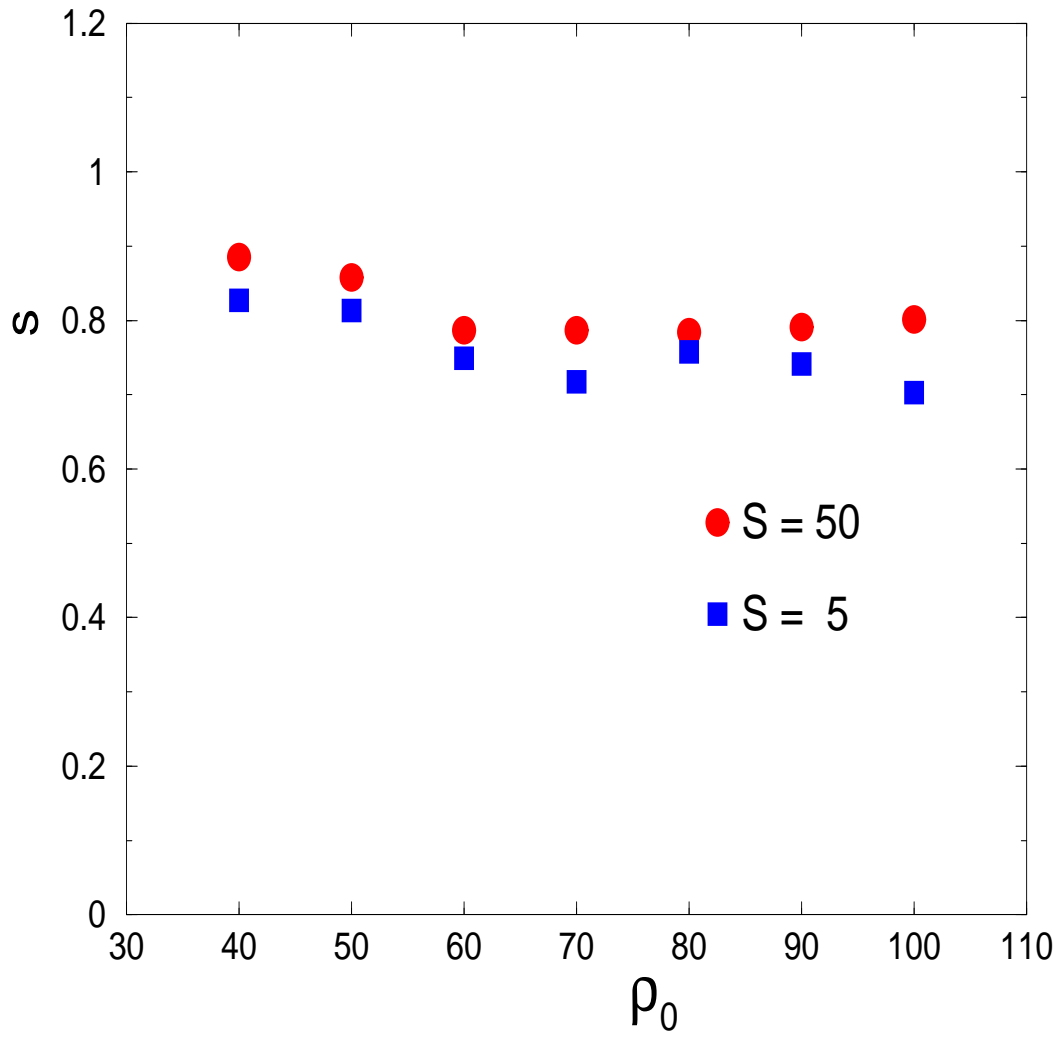


Fig.6